AN ACTIVE BREATHING WALL TO IMPROVE INDOOR ENVIRONMENT

Yue Zhao[1], Tengfei (Tim) Zhang[1], Shugang Wang[1], and Yang Geng[2]
[1]School of Civil Engineering, Dalian University of Technology (DUT)
2 Linggong Rd, Dalian 116024, China
[2]School of Architecture and Fine Art, Dalian University of Technology (DUT)
2 Linggong Rd, Dalian 116024, China

ABSTRACT

To maintain good indoor air quality, this investigation proposes a prototype of an active breathing wall system, which is composed of a solar radiation absorption board, air heating cavity, porous filtration unit and fan device. The thermo-flow performance of a physical model is measured and compared against the computational fluid dynamics (CFD) modeling. Then an office environment with a breathing wall is simulated by CFD. This study finds different ventilation modes are formed within the room in different seasons. The system generally has good performance to enhance the outdoor air supply rate without causing moisture condensation in the winter.

INTRODUCTION

To conserve energy, modern buildings are designed to hold better air tightness. Most commercial buildings are equipped with mechanical ventilation, so the outdoor fresh air may only be introduced into indoor space through ventilation. For residential buildings which use natural ventilation, doors or windows shall be opened when outdoor air is needed. However, this can cause problems in dense towns or cities, because the outdoor noise and polluted traffic air may also be imported into the space if doors or windows are open. The appearance of breathing walls seems to provide a good solution to the dilemma. A breathing wall which contains a porous filtration unit can block the outdoor noise and filter the air permeating into the indoor space. However, the breathing wall shall be carefully designed to ensure its good performance.

A breathing wall is also called dynamic insulation, through which the indoor and outdoor air is exchanged via air permeation through porous material. The earliest relevant concept was developed in 1960s, when the agricultural buildings were constructed using dynamically insulated ceilings (Graee, 1974). Since the late 20th century, Taylor and Imbabi (1996) carried out extensive research on breathing walls. The breathing wall is found being able to improve indoor health but still hold good energy efficiency (Imbabi, 2006). As the breathing wall is composed of porous unit that behaves as a filter (Taylor et al., 1999), most of coarse particles travelling together with the air can be removed. The outdoor air permeating through the breathing wall has an opposite direction with the heat loss, so most of the conduction heat loss can be recovered and thus providing good insulation. For example, if there is air penetrating into indoors in the winter, the penetrative air gets heated by the conduction heat loss within the breathing wall. Since the penetrative air is finally delivered to the indoor space, the breathing wall would recover the energy that originally would be lost to the outside if using a traditional solid wall.

The above breathing wall sounds flawless; however, it may not work well if the following problems are not resolved. First, the aforementioned breathing wall can only provide dynamic insulation when the air permeates in a unique direction that should be opposite to the heat loss. If unfortunately there are cracks on the building envelopes, such as a small joint clearance in the windows or doors, the air will bypass the breathing wall because of larger flow resistance (Baker, 2003; Dimoudi et al, 2004). Second, the air permeation through a breathing wall is subject to the outdoor wind that is essentially chaotic in direction and strength. This makes hard to assure the expected moving direction of penetrative air. Finally, if the outdoor air temperature is extremely low in the winter, the penetrative outdoor air will result in low temperature of indoor space (Gan, 2000), which may be far from the comfortable range. In addition, the created low room surface temperature imposes great risks in condensing moisture in indoor spaces (Yoon and Hoyano, 1998).

The above review reveals that although a breathing wall seems promising to conserve energy and improve indoor environment, the traditional passive breathing scheme may not work well. This investigation has thus proposed to design an active breathing wall by installing a fan inside the wall to remedy the existent problems. Such a breathing wall system is promising to be applied in dense city downtowns to improve air quality and keep indoor space quietly. In addition, the breathing wall is coupled together with an indoor space to fully evaluate the performance of the system using computational fluid dynamics (CFD) modeling.

THE BREATHING WALL SYSTEM

The designed breathing wall system as shown in Figure 1 is composed of frame, glass panel, solar radiation absorption board, air cavity, porous filtration unit, cross-flow fan, muffler, and air discharge vent. The flow schemes for winter and summer use are slightly different. The outdoor air is drawn into the cavity from the bottom air intake.

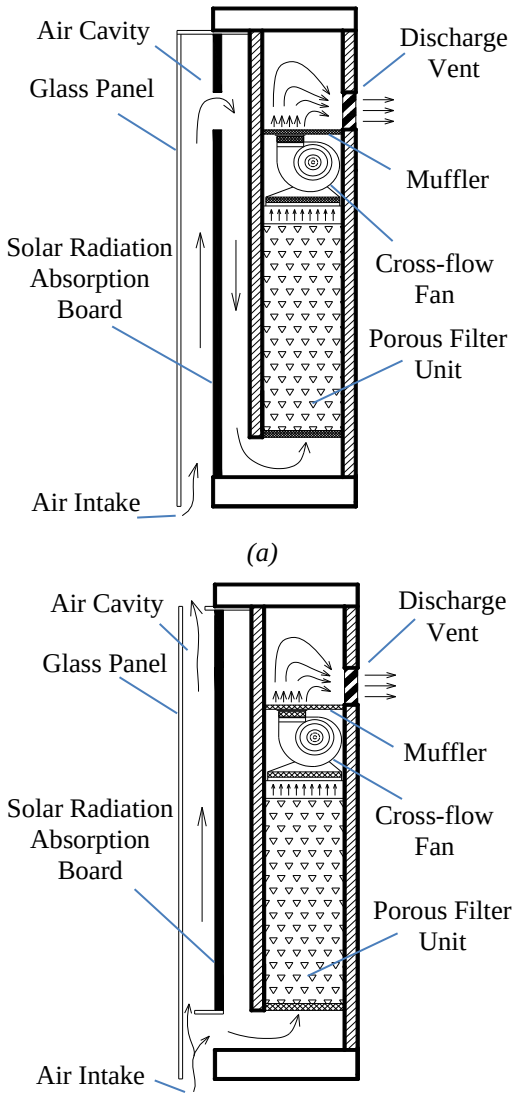

Figure 1 Side view of the designed scheme of an active breathing wall. (a) for winter use, (b) for summer use

If there is solar radiation in the winter as shown in Figure 1(a), the solar radiation absorption board keeps a higher temperature than the air, so the air inside the cavity gets heated. The heated air rises up due to thermal buoyancy and enters into the space behind the board. Then the air is guided to go down, which forms a zigzag flow path. Such design will be helpful for depositing and removing the coarse particles. Afterward, the air goes up again and permeates through the porous filtration unit, and fine particles are filtered therein. In case the solar radiation is not strong enough to drive air motion, a cross-flow fan is installed above the filtration unit. Before the air is discharged out, a fire-resistant muffler is designed to insulate the fan noise. In the summer season, the flow path is simpler as shown in Figure 1(b). To prevent introducing hot air to the indoor space, the top cover of the air cavity is removed, and the cavity behaves as a chimney. The induced air is guided into the wall and then directly drawn up to permeate through the porous filtration unit.

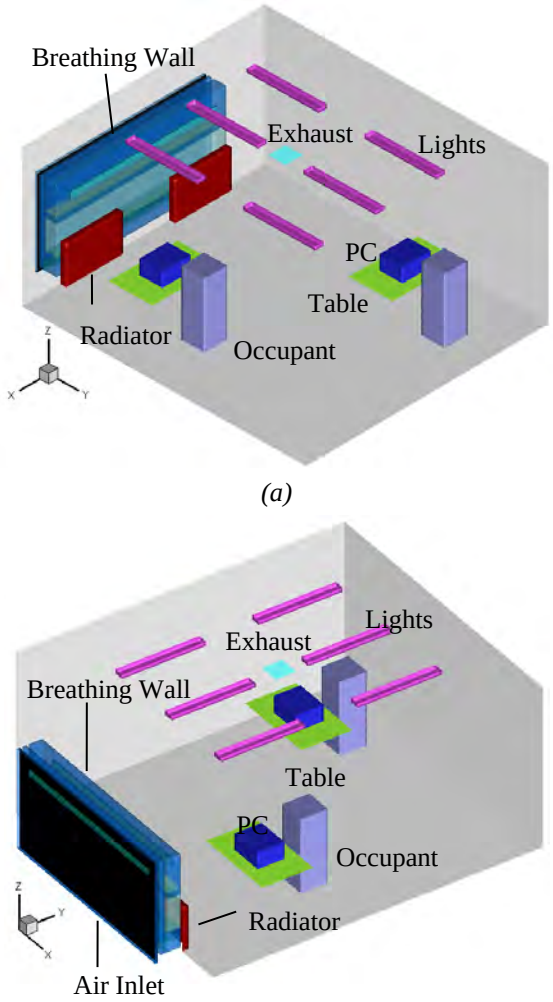

Figure 2 Layout of an office with the breathing wall system: (a) inside view, (b) outside view

To evaluate the breathing wall performance, it is installed to the envelope wall of an office room neiboring to the outside as shown in Figure 2. The room dimensions are 4.32m × 4.92m × 2.42m. Six fluorescent lamps are mounted on the ceiling to provide illumination. There are two occupants seating sedentarily before a computer simulator on the table. Suppose there is no mechanical ventilation,

Table 1
Boundary conditions for the breathing wall system

Parameters	Breathing wall system	
	Winter Use	**Summer Use**
Outdoor air temperature (℃)	-5	30
Supply air rate to the room (l/s)	37	37
Fan pressure rise (Pa)	20	20
Heat release by the absorption board (W/m^2)	212.5	173.4
Porosity of the porous filtration material	0.1	0.1
Viscous resistance of the porous media	5.0E+07	5.0E+07
Inertial resistance of the porous media	1400	1400
Heat release by the radiators (W)	320	0
Temperature of the chilled ceiling (℃)	adiabatic	15
Other room surface	adiabatic	adiabatic
Room exhaust outlet	zero pressure	zero pressure

and the outdoor air is only provided by the breathing wall, which is located at the lower part of the envelope wall. The breathing wall has dimensions of 3.0m×0.5m×1.5m. In front of the breathing wall, there are two radiators, and would put operation in the winter season. A square exhaust outlet is placed on the central ceiling to extract the room contaminated air.

Table 1 lists boundary conditions of the breathing wall system together with the office room. The outdoor air temperature is -5 ^{o}C for winter and 30 ^{o}C in summer. The sun irradiation intensity is not set identical between the winter and summer. To prevent overheating within the air cavity, the glass panel is coated by white paint in the summer season. This is why the heat released by the absorption board in the summer case is a little lower than that of the winter case. Air flow rate to the room is designed to be 37 l/s regardless of the season. The pressure jump by the fan is 20 Pa to provide the required air rate. Note, the breathing wall is not an air conditioner, so the thermal condition of the room should be controlled by other methods. In winter, the radiator should put operation and the heating power is assumed to be 320 W. While in summer, the whole ceiling is cooled by the chilled beam with a temperature of 15 ^{o}C. For simplicity, other surfaces of the office room are assumed to be adiabatic.

To examine the validity of the breathing wall system and evaluate the created indoor environmental conditions, the thermo-flow parameters including air velocity and temperature within both the breathing wall and office are solved. Because indoor air flow is generally turbulent, turbulence modeling is required. This investigation adopts the Re-Normalization Group (RNG) k-ε model based on the RANS (by solving the Reynolds-averaged Navier-Stokes equations) CFD approach. There are hugely different dimensional scales in the studied environment. The smallest scale is in the filtration unit, which can be as small as several milimeters if the granular bed or fiber filter is used for air filtration. While, in the room it spans several meters. The CFD simulation might have difficulty in modeling the multi-scale flow phenomena if they are not treated appropriately. This paper models the flow permeating through the filtration unit based on the volumetirc average method (Vafai, 2000), since only the mean parameters are of concern. Therefore, the governing equation within the porous media is similar to the pure fluid, except for the additional flow resistance exerted by the solid phase. The viscous and inertial resistance are shown in Table 1. The porosity of the filtration material is 0.1.

The geometry of the studied cases is created by GAMBIT and then suitable CFD meshes are generated. The breathing wall is meshed into the quad grids with a size of 2.5 cm using the Map scheme. Unstructured tetrahedral grids are created in the office with the Tet/Hybrid scheme. A grid size function is employed to shift the grid size gradually from 3 cm near the occupants and discharge vent to 7.5 cm inside the room. The total grid cell number for the winter case is 1.45 million, and for the summer case 1.43 million. Then the CFD grid cells are imported into FLUENT for flow and temperature simulation. The discretization scheme for pressure is the pressure staggering option (PRESTO), which can fully take into account the thermal buoyancy. While, the discretization for momentum, turbulent kinetic energy, turbulent dissipation rate and energy is the second-order upwind scheme. Finally, the continuity equation is coupled with the momentum equation via the SIMPLE algorithm for flow solution.

VALIDATION OF CFD MODELING

Because this investigation mainly apply CFD modeling as the research tool, it is necessary to validate the numerical modeling. The RANS CFD modeling employes a significant number of

assumptions, which may result solution uncertainty. Such uncertainty shall be quantitatively identified in the research.

(a)

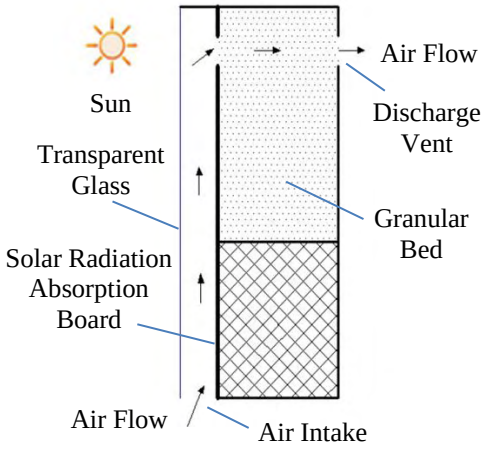

(b)

Figure 3 The breathing wall used for numerical modelling validation: (a) picture of the test facility, (b) schematics of the working principle

The validation procedure conducted experimental test of a simplified breathing wall as shown in Figure 3. The breathing wall has dimensions of 1.5m × 0.5m × 1.2m. For construction convenience, the breathing wall did not take the same design as that shown in Figure 1. There is no fan to impel the air permeation, so the air motion is only driven by the natural convection flow induced by the solar radiation. The flow path is designed into along only one direction as shown in Figure 3(b). A granular bed which is filled by dielectric particles with a mean diameter of 3.5 mm, is employed to filter the penetrative air. The porosity of the granular bed is 0.1.

The breathing wall device is exposed to a nearly static ambient environment at around 10 ^{o}C. An array of tungsten lamps are applied to mimic the solar radiation (Figure 3(a)). The mean temperature of the solar board is around 70 ^{o}C. An ultrasonic anemometer (type DA-650&TR-92T; Kaijo Sonic, Japan) is applied to measure the air speeds at the air intake and discharge vent. The resolution of the anemometer is 0.005m/s with 1% uncertainty for velocity measurement. In addition, the temperatures at 16 different points are measured by a thermometer with Pt-100 as sensor probes. The temperature reading is fulfiled by a Keithley data acquisition system (type 2700; Keithley Instruments, USA), which has a resolution of 0.15 ^{o}C with 0.1% measurement uncertainty.

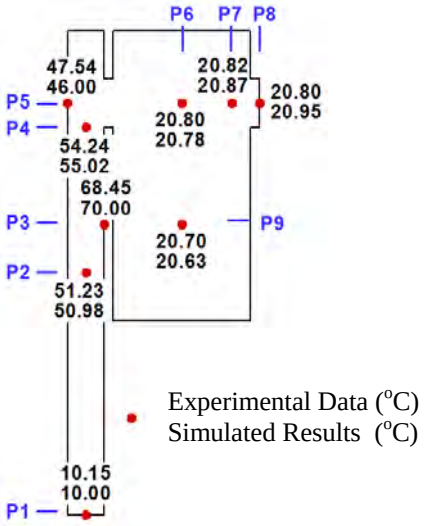

Figure 4 Comparison of the measured and CFD computed temperature with the breathing wall

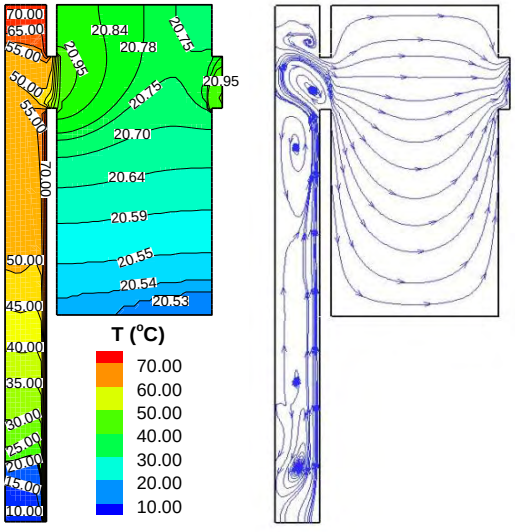

(a) *(b)*

Figure 5 CFD simulated temperature distribution and flow pathline in the breathing wall for numerical validation: (a) air temperature distribution, (b) flow streamline

After the experimental test, the whole case is reproduced by CFD modeling. Only the breathing wall itself is modelled excluding the ambient air environment. The air intake is set as a pressure-inlet

and the discharge vent is a pressure-outlet. Structured grid meshes were created using the Hex/Map scheme. The total grid number is 84,440. Other CFD settings are similar to those described in the previous section.

Figure 4 shows the comparison of temperature between the CFD simulation and the measurement only at 9 different positions. Because of the rejected heat by the solar board, the temperature inside the cavity increases steadily. The heated air exchanges heat with the granular bed and drops to around 21 ^{o}C. Since the envelope surfaces of the breathing wall are not well insulated, it is very hard to keep the same high temperature when the air discharges. P5 is on the glass panel, so the temperature is low. From the comparison, the computed temperature by CFD is higher or lower than the measurement within 2 ^{o}C. This shows the CFD simulation has obtained reasonably good accuracy. The simulated distribution of air temperature and flow pathline can also be observed in Figure 5.

Besides, the average air speed at the discharge vent is also compared between the CFD and measurement. The CFD computed an air speed of 0.2 m/s at the discharge vent, where the measurement obtains 0.15 m/s. Because the velocity is very low, there is also uncertainty in measurement itself. This investigation thus concludes the CFD modeling has obtained reasonably good results in consistency with the measurement. Although the validated breathing wall has a different design with that ultimately proposed for the office environment, the underlying flow and heat transfer principles are the same. Therefore, CFD can be used to evaluate the breathing wall system performance.

RESULTS

After validating the numerical procedure, the CFD is further applied to solve the thermo-flow conditions inside the office room. Figure 6 shows the simulated temperature distribution in the office for the winter season. Three typical planes along the X direction are selected, which are across the two occupants and the mid section, respectively. The outdoor air temperature is -5 ^{o}C, but after being heated in the breathing wall, the temperature at the discharge vent increases to 18 ^{o}C. As the discharged air temperature is still lower than the average room temperature (22 ^{o}C), there is no surprise to see the temperature gradient within. In general, the floor is maintained at 20 ^{o}C and then the temperature gradually rises to 24 ^{o}C near the ceiling. The temperature gradient is controlled within 2 ^{o}C/m, so there is minimal risk in imposing draught complaint.

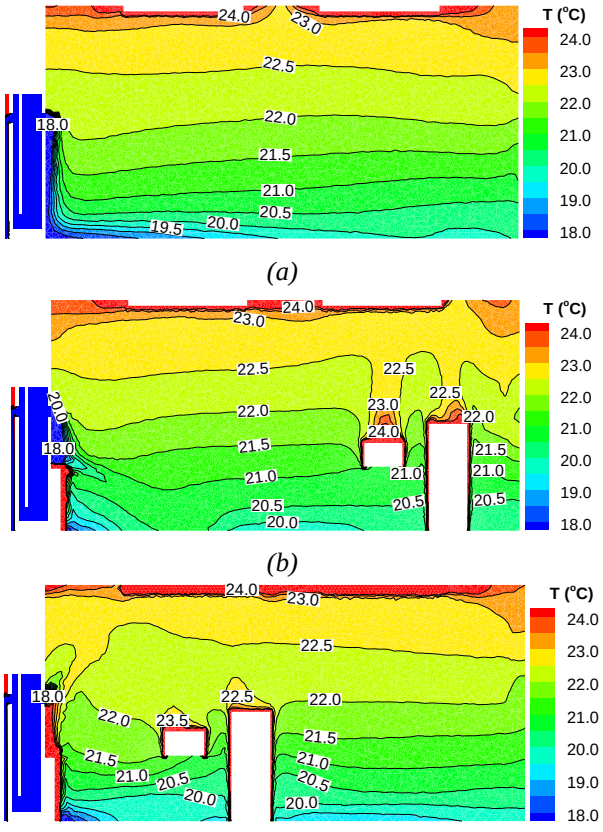

Figure 6 Temperature distribution of the office with a breathing wall for winter use: (a) X=1.15 m, (b) X=2.15 m (middle), (c) X=3.15m

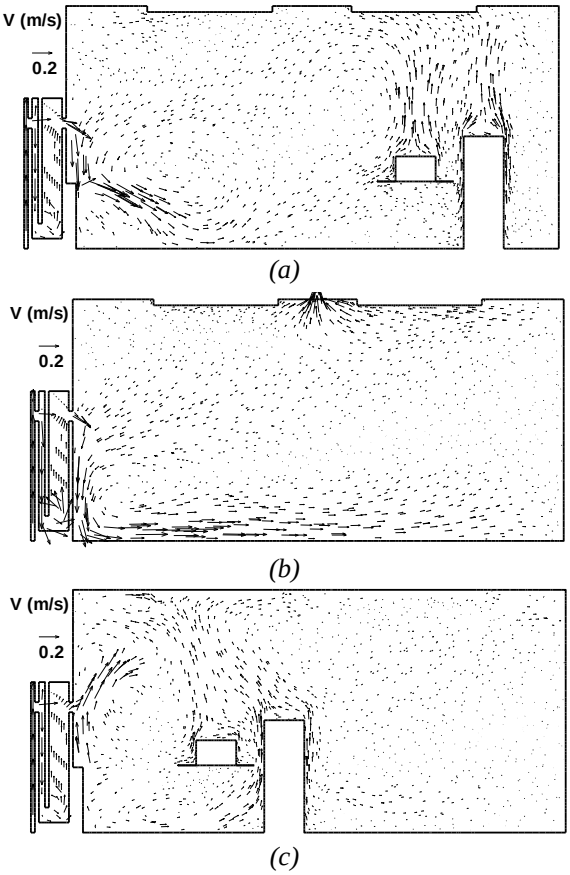

Figure 7 Velocity distribution of the office: (a) X=1.15m, (b) X=2.15 m (middle), (c) X=3.15 m

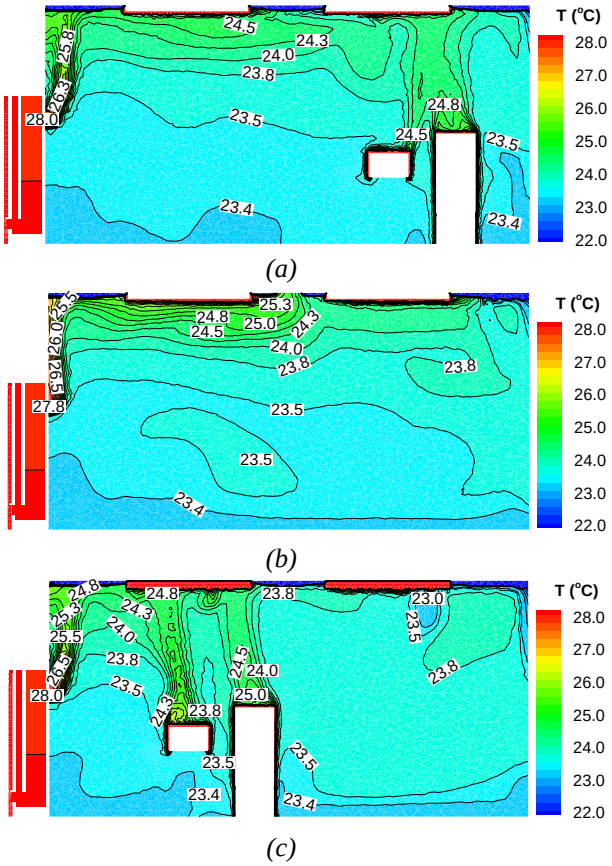

Figure 8 Temperature distribution of the office with a breathing wall for summer use: (a) X=1.15m, (b) X=2.15 m (middle), (c) X=3.15m

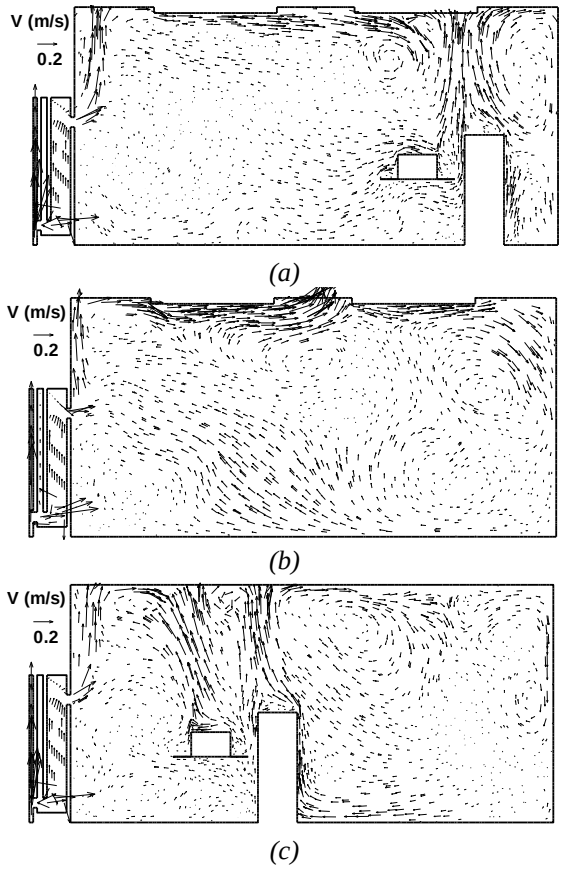

Figure 9 Velocity distribution of the office for summer use: (a) X=1.15m, (b) X=2.15 m (middle), (c)X=3.15 m

As the planes of X=1.15 m (Figure 6(a)) and 3.15 m (Figure 6(c)) are across the two radiators, the high temperature near the radiator can be viewed. The radiator drives the discharged air from the breathing wall rising up as shown in Figure 7(c) but not Figure 7(a). This is because X=1.15 m is just across the edge of the radiator rather than in the middle as that in Figure 7(c). In the mid section of the room (Figure 7(b)), the discharged air from the breathing wall also drops to the ground due to lower air temperature than the surrounding. The temperature stratification and the dropping-down flow pattern highlights that the breathing wall for the winter use has created a ventilation mode similar to the displacement ventilation. The mixing extent of the air for the winter use is small, which would be helpful for maintaining good indoor air quality. However, the presence of radiators seems to counteract the displacement ventilation effect. The lowest temperature on the room surfaces is 15.2 ^{o}C. If the relative humidity of indoor air is lower than 40%, there is no risk for moisture condensing on the surface.

Figure 8 shows the temperature distribution when the breathing wall is used in the summer season. The hot air at around 30 ^{o}C after entering into the air intake of the breathing wall is divided into two streams. One stream goes upward through the cavity because of the solar chimney effect. The other stream is driven by the fan and supplied to the room after sweeping through the porous unit. As the room is cooled down by the whole chilled ceiling (15 ^{o}C), the room air temperature is quite uniform at an average 23.5 ^{o}C. The porous unit is also cooled somehow by the room, so the air temperature at the discharge vent is a little bit lower than the outside air temperature. The air provided by the breathing wall quickly rises up along the side office wall, so the flow inside the room is complicated as shown in Figure 9. In general, the flow features and temperature distribution are quite similar to the mixing ventilation. Therefore, the ventilation effectiveness for the summer use is poorer than that for the winter use.

CONCLUSIONS

This paper proposes an active breathing wall by equipping a fan inside the wall, which makes the device workable regardless of the outdoor season conditions. An air cavity is designed which can heat the air in the winter season, but behaves as a chimney to induce air motion in the summer. By installing the breathing wall into an office room and evaluating the performance with CFD modeling, it finds different thermo-flow conditions are created in summer and

winter. In the winter, the created ventilation mode is close to the displacement ventilation, which is helpful for maintaining good air quality. However, the presence of radiators counteracts the effect by the displacement ventilation. If the relative humidity of indoor air is lower than 40%, there should be without risk to condense moisture within the room. When the breathing wall is used in the summer, it creates a ventilation mode similar to the mixing ventilation.

ACKNOWLEDGEMENT

This research work was supported by the National Natural Science Foundation of China (Grant No.: 50978039).

REFERENCE

Baker, P.H. 2003. The thermal performance of a prototype dynamically insulated wall, Building Service Engineering Research and Technology, 24(1), 25-34.

Dimoudi, A., Androutsopoulos, A., Lykoudis, S. 2004. Experimental work on a linked, dynamic and ventilated, wall component, Energy and Buildings, 36, 443-453.

Gan G. 2000. Numerical evaluation of thermal comfort in rooms with dynamic insulation, Building and Environment, 35, 445-453.

Graee, T. 1974. Breathing building construction, Oklahoma, ASEA Stillwater.

Imbabi, M.S. 2006. Modular breathing panels for energy efficient, healthy building construction, Renewable Energy, 31, 729-738.

Taylor B.J., Webster R., Imbabi, M.S. 1999. The building envelope as an air filter, Building and Environment, 34, 353-361.

Taylor, B.J., Cawthorne, D.A., Imbabi, M.S. 1996. Analytical investigation of the steady-state behaviour of dynamic and diffusive building envelopes, Building and Environment, 31(6), 519-525.

Yoon, S., Hoyano, A. 1998. Passive ventilation system that incorporates a pitched roof constructed of breathing walls for use in a passive solar house, Solar Energy, 64(4-6), 189-195.

Vafai, K. 2000. Handbook of porous media, New York, USA: Marcel Dekker, Inc..